Available online at www.sciencedirect.com
ScienceDirect
Journal of the European Ceramic Society 31 (2011) 2319–2329
www.elsevier.com/locate/jeurceramsoc

Glycothermal process for barium magnesium tantalate nanopowders synthesis

Amar Badrakh [a], Hyun-Sig Kil [a], Dae-Young Lim [a,b], Seung-Beom Cho [c,*], Sahn Nahm [d], Richard E. Riman [e]

[a] Department of Materials Engineering, Graduate School of PaiChai University, Daejeon, South Korea
[b] Department of Information & Electronic Materials Engineering, College of Engineering, PaiChai University, Daejeon, South Korea
[c] Information Technology & Electronic Materials R&D, Research Park, LG Chem. Ltd., Daejeon, South Korea
[d] Department of Materials Science and Engineering, Korea University, Seoul, South Korea
[e] Department of Materials Science and Engineering, Rutgers, The State University of New Jersey, Piscataway, NJ 08855-0909, United States

Received 23 December 2010; received in revised form 17 May 2011; accepted 25 May 2011

Abstract

Barium magnesium tantalate $Ba(Mg_{1/3}Ta_{2/3})O_3$ (BMT) nanopowders were synthesized at a low temperature of 220 °C through glycothermal reaction by using $Ba(OH)_2{\cdot}8H_2O$, $Mg(NO_3){\cdot}6H_2O$, and $TaCl_5$ as precursors and 1,4-butanediol as solvent. It is demonstrated that higher synthesis temperatures and co-precipitation of magnesium and tantalum improve the incorporation of magnesium into BMT nanopowders under glycothermal treatment and produce a homogeneous, stoichiometric powder. The glycothermally derived BMT nanopowders are very reactive and provide a high-density sintered body with 97.1% of theoretical density at a low temperature of 1350 °C. The average grain size of the sintered ceramics was 1.2 ± 0.2 μm and relatively uniform in comparison with the ceramics sintered with powders produced from the conventional method.

Keywords: Glycothermal; A. Powders-chemical preparation; A. Sintering; D. Perovskites; D. Tantalates

1. Introduction

The demand for microwave dielectric resonators is rapidly rising as communication systems depend on more and more on microwave technology. The three key requirements for a dielectric resonator are a high dielectric constant, K for possible miniaturization (because the size of a dielectric resonator $1/\tan\delta$, a high unloaded dielectric loss (high $Q \times f$ value) for a stable resonant frequency where Q is equal to $1/\tan\delta$ and f is the measuring frequency, and a near-zero temperature coefficient of resonant frequency (TCF) for temperature-stable circuits.[1] To satisfy the demands of microwave circuit designs, each dielectric property should be precisely controlled.

Several complex perovskite ceramics $Ba(B_{1/3}B'_{2/3})O_3$ where B = Zn or Mg and B′ = Nb or Ta have been reported due to their remarkable microwave dielectric properties, which include a high K ($\varepsilon_r \sim 23$–25), a small TCF ($\tau_f \sim 2.7$–7.5), and especially the highest quality factor ($Q \times f$ value ~150,000–200,000 GHz) ever known for a perovskite material.[2–6] Therefore, these materials are commonly used in microwave devices such as dielectric resonators, filters, duplexers, mixers, global positioning systems, voltage-controlled oscillators, and antennas. To satisfy the demands of microwave circuit designs, each dielectric property should be precisely controlled.[7–13] Dielectric losses in microwave frequencies are related to the degree of B-site ordering, porosity, secondary phases, and crystal imperfections in ceramics.[14,15]

The usual process of preparing BMT-based materials by solid-state reaction of $BaCO_3$, MgO and TaO, are currently most suitable for the industrial production of ceramic dielectric resonators. A significant problem concerning the conventional solid-state reaction is that very high temperatures are needed for the sintering (≥1600 °C) and the BMT powder also has poor sinterability. Furthermore, the complete ordering between B site ions requires extremely long annealing times (100 h). This has been a serious problem in the practical applications of the present

* Corresponding author. Tel.: +82 42 866 2415; fax: +82 42 862 6073.
E-mail address: sebcho@lgchem.com (S.-B. Cho).

0955-2219/$ – see front matter © 2011 Elsevier Ltd. All rights reserved.
doi:10.1016/j.jeurceramsoc.2011.05.038

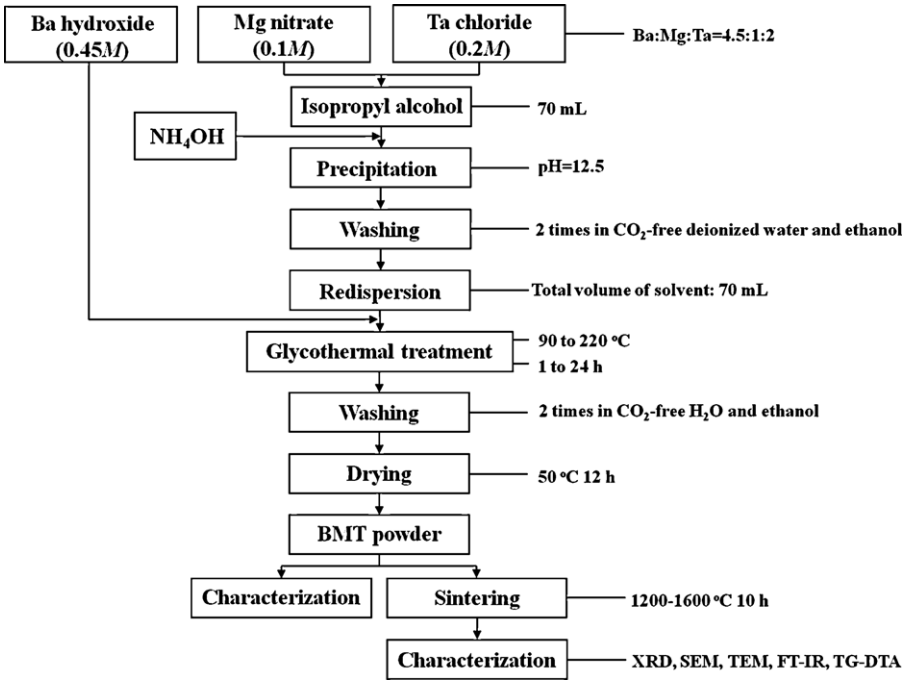

Fig. 1. Schematic representation of processing steps for the preparation of $Ba(Mg_{1/3}Ta_{2/3})O_3$ nanoparticles via glycothermal process.

ceramics. In general, the Q value of BMT ceramics significantly depends on the compositional purity, sintering density, and the degree of ordering of magnesium and tantalum cations locating in B-sites.[16]

Many efforts had been tried to create dense BMT ceramics at lower temperatures. Two methods are commonly used for reducing the sintering temperature of BMT ceramics, namely low melting sintering aid[17] and chemical solution processing of the starting ceramic powers.[18] Generally, low melting sintering aids compromise the microwave dielectric properties.[11] Wet chemical solution routes have proven to be more effective for improving sinterability and reproducibility because these chemical solution synthesis routes produce very pure, homogeneous, and extremely fine ceramic powder. Moreover, high sinterability and high reproducibility are generally important for the dielectric materials prepared by wet chemical solution methods.[19,20]

The need for the close control of ceramic powders characteristics has directed attention to solvothermal synthesis technique.[21] Solvothermal methods are useful for the precipitation of ceramic powder of fine particle size and uniform morphology in a single experimental step at moderate temperatures and pressures. This process leads to powders with high chemical and phase purity and a small degree of aggregation and agglomeration. The success of solvothermal synthesis depend on the selection of precursors that are both reactive and cost effective as well as choosing the appropriate process conditions, which include temperature, pH, reagent concentrations, and solvent environment.[22]

Recently, use of diols for inorganic synthesis has attracted much attention.[23] To our knowledge, no studies on the glycothermal synthesis of crystalline $Ba(Mg_{1/3}Ta_{2/3})O_3$ powders have been reported. Compared to conventional hydrothermal processing techniques which use water as a solvent, glycothermal methods have many advantages. First, glycothermal method does not need an inorganic mineralizer for the formation of anhydrous crystalline materials in some cases because 1,4-butanediol can complex ions to promote solubility. Avoiding the inorganic mineralizers prevent contamination by alkalis and/or halides, which are commonly used in conventional hydrothermal process. Second, glycothermal method significantly reduces the reaction pressure, enabling the use of large reactors that operates at low pressure. Third, glycothermal media offers facile control of size and morphology without the need for growth-directing agents.[24–26]

The objective of this paper is to develop a new glycothermal process to synthesize crystalline $Ba(Mg_{1/3}Ta_{2/3})O_3$ powder, using 1,4-butanediol as solvent. The present work will demonstrate has three major advantages; namely, stoichiometric control, mild glycothermal reaction conditions, and low sintering temperatures.

2. Experimental procedure

2.1. Glycothermal synthesis

A flow chart illustrating the overall glycothermal method of BMT synthesis is shown in Fig. 1. Barium hydroxide octahydrate, $Ba(OH)_2{\cdot}8H_2O$ (99%, JUNSEI Chemical. Co., EP, Tokyo, Japan), was used as received. Magnesium nitrate, $Mg(NO_3)_2{\cdot}6H_2O$ (99%, YAKURl Chemical, Co., EP, Osaka, Japan), and tantalum pentachloride, $TaCl_5$ (99.8%, KISAN KINZOKU Chemicals, Osaka, Japan), was used as a source of magnesium and tantalum, respectively. Magnesium and tantalum were added in the form of a co-precipitated hydrous double oxide $Mg_xTa_{(1-x)}O_2{\cdot}nH_2O$ (MTO, $x = 1/3$). Stoichio-

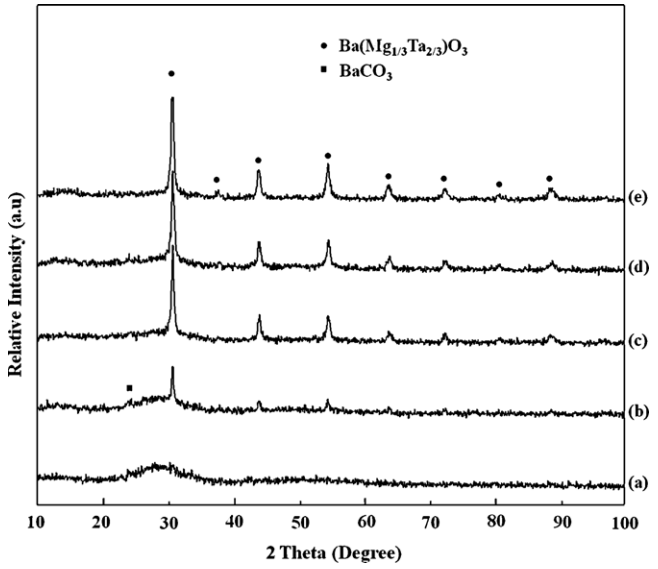

Fig. 2. XRD patterns of $Ba(Mg_{1/3}Ta_{2/3})O_3$ nanopowders synthesized in glycothermal condition at various reaction temperatures (24 h, Ba:Mg:Ta molar ratio of 1.5:0.33:0.67): (a) 90 °C, (b) 120 °C, (c) 150 °C, (d) 180 °C, and (e) 220 °C.

metric amounts of magnesium nitrate and tantalum chloride were dissolved in 70 mL 2-propanol (Fisher Scientific, histological grade, Pittsburgh, PA, USA) to obtain a stable solution because $TaCl_5$ is readily hydrolyzed by reacting with water from air. Subsequent hydrolysis of this solution at room temperature by 1 M NH_4OH solution produced a co-precipitated MTO gel. The MTO gel was separated and washed with CO_2-free deionized water and ethyl alcohol by three cycles of centrifugation for 4 min at 5000 rpm in a centrifuge (Beckman Induction Drive Centrifuge, Model J2-21 M, Beckman Instruments, Fullerton, CA, USA). Redispersion of gel sediment was

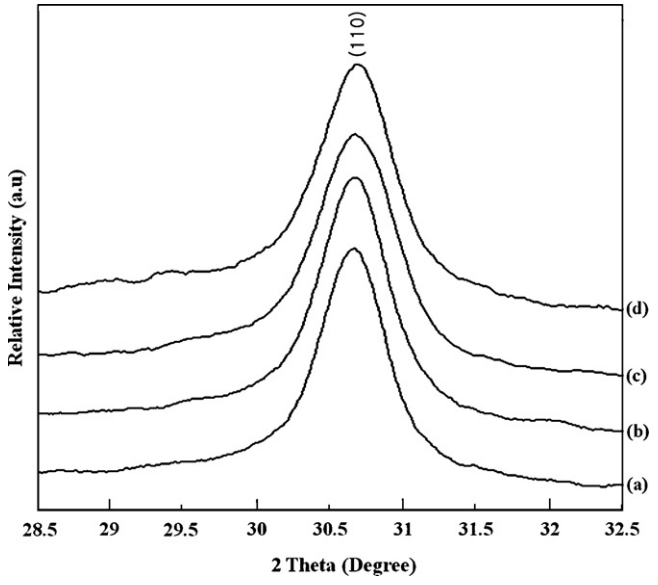

Fig. 3. XRD patterns of the (1 1 0) reflections of $Ba(Mg_{1/3}Ta_{2/3})O_3$ nanopowders synthesized in glycothermal condition at various reaction temperatures (24 h, Ba:Mg:Ta molar ratio of 1.5:0.33:0.67): (a) 120 °C, (b) 150 °C, (c) 180 °C, and (d) 220 °C.

Table 1
Crystallite size of $Ba(Mg_{1/3}Ta_{2/3})O_3$ nanopowders synthesized in glycothermal condition at various reaction temperatures (24 h, Ba:Mg:Ta molar ratio of 1.5:0.33:0.67).

Sample #	Reaction temperature (°C)	Crystal size (nm)
BMT-1	90	–
BMT-2	120	10.1
BMT-3	150	15.4
BMT-4	180	16.7
BMT-5	220	19.7

performed with Thermolyne Maxi Mix II, type 37600 mixer (Bamstead/Thennolyne, Dubuque, IA, USA). Excess ethyl alcohol was decanted after final washing and wet precursors was redispersed in 1,4-butanediol solution (99%, Aldrich Chemical). $Ba(OH)_2{\cdot}8H_2O$ was then added into 1,4-butanediol. Total solvent volume was 70 mL. In all runs, a MTO concentration of 0.1 M and a Ba/(Mg + Ta) ratio of 1.5 were employed. To investigate the effects of reaction temperature on phase and morphology of BMT nanopowder in glycothermal condition, reactions were carried out at temperatures from 90 to 220 °C. The resulting suspension was placed in a 125 mL stainless-steel Teflon-lined autoclave (Large Capacity Acid Digestion Bomb, Parr Instruments, Moline, IL, USA) with a fill factor of 65 vol.%. The Teflon-lined vessel was flushed with nitrogen before closing.

The reaction vessel was then heated to the desired temperature (90–220 °C) with a rate of 2 °C/min. The reaction time at the desired temperature was 24 h. After glycothermal treatment, the vessel was cooled to ~40 °C. The powders were washed with pH adjusted (pH ~ 10) CO_2-free deionized water to remove the unreacted Ba in solution, and also prevent incongruent dissolution of the barium ions from the BMT powder surface via formation of $BaCO_3$.[27] The recovered BMT nanopowders were dried at 50 °C in a desiccator for 24 h. To investigate the effects of reaction temperature on the formation of stoichiometric BMT nanopowder in glycothermal condition, as-synthesized BMT nanopowders were calcined from 600 to 1100 °C with temperature interval of 100 °C in an alumina crucible in air for 4 h. The optimum calcination temperature was determined as 1100 °C for 4 h which was the lowest temperature to confirm the formation of phase-pure BMT powder without any second phase.

2.2. Characterization

Phase composition and crystal structure were analyzed using X-ray diffraction (XRD, Cu $K_{\alpha 1}$, Fine Tube, 40 kV to 40 mA, Rigaku, Tokyo, Japan) over the 2θ range from 10° to 100° at a scan rate of 2°/min. The crystallite size of BMT nanopowder, D, was calculated from the broadening of (1 1 0) XRD main peak using the Scherrer formula[28]:

$$D = \frac{0.94\lambda}{\beta \cos\theta}$$

where D is the crystallite size, λ (=0.15406 nm) the wavelength, β the true full width at half maximum and θ the diffraction angle of the center of the peak (in degrees). The morphology

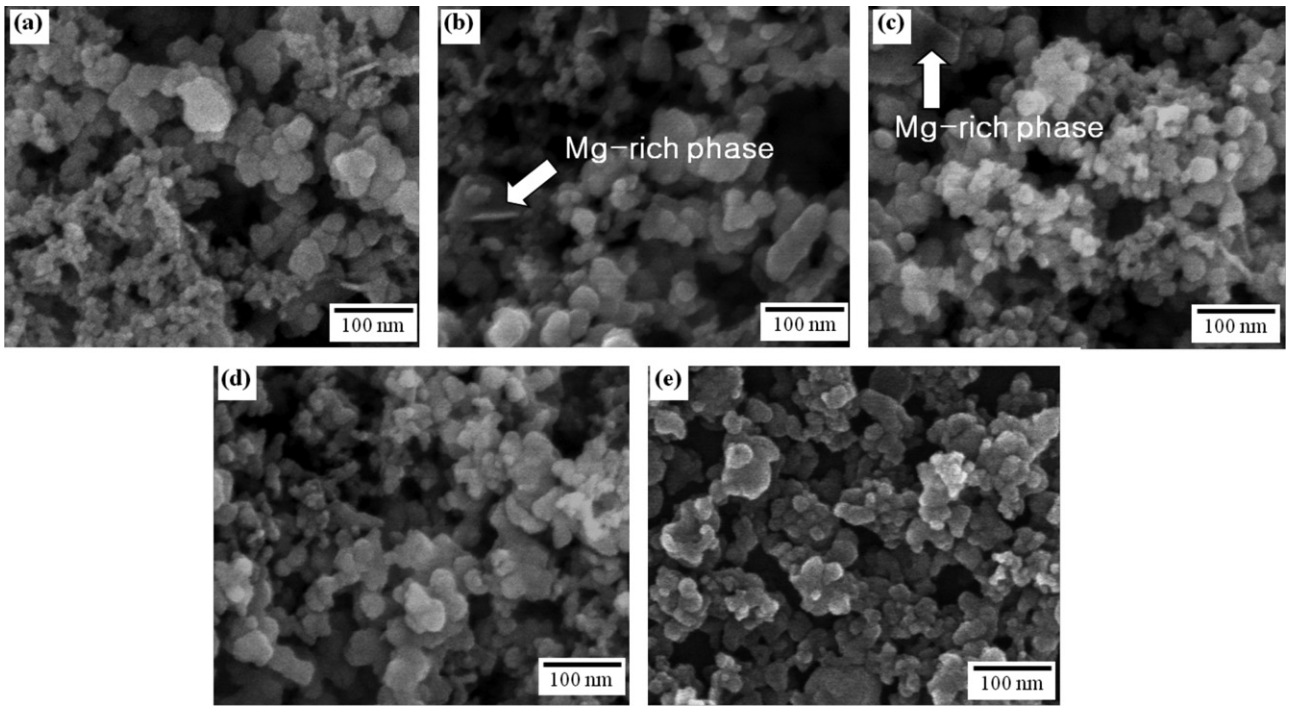

Fig. 4. SEM photomicrographs of $Ba(Mg_{1/3}Ta_{2/3})O_3$ nanopowders synthesized in glycothermal condition at various reaction temperatures (24 h, Ba:Mg:Ta molar ratio of 1.5:0.33:0.67): (a) 90 °C, (b) 120 °C, (c) 150 °C, (d) 180 °C, and (e) 220 °C.

of the synthesized particles was observed using field-emission scanning electron microscopy (FESEM, S-4200, Hitachi, Tokyo, Japan) and transmission electron microscopy (TEM, JEM-2000-EX II, JEOL, Tokyo, Japan). Qualitative analysis using EDS analysis were accumulated over the range of 0–40 keV using channels 20.83 eV wide, a beam size 8.8 nm, and a residence time of 200 s. High resolution lattice images also were taken to confirm crystallinity. Infrared absorption was measured using Fourier transform infrared (FTIR) spectrophotometer (Model FTIR 8700, Shimadzu Co., Kyoto, Japan) for analysis of surface impurities on BMT nanopowders such as C–O and O–H groups and carbonates using the KBr pellet technique. IR samples were prepared by mixing dry precipitate with dry KBr in 1:100 ratio by weight. The materials were ground by hand in an agate mortar and pestle and pressed in mold for 5 min with holding. Thermogravimetric analysis (TGA) was carried out to understand the decomposition and synthesis process and to optimize the calcination temperature. Thermogravimetric analysis (TGA) was performed with heating rate of 2 °C/min up to 1200 °C.

Cylindrical (Ø = 13 mm × 1 mm) ceramic bodies were shaped by uniaxial pressing the BMT powders at 150 MPa and sintering in air at 1200–1600 °C for 10 h. The bulk density of the sintered pellets was measured using Archimedes method, where the value of 7.626 g/cm^3 is used as the theoretical density of BMT. The sintered samples were thermally etched at 1200 °C for 3 h in alumina crucible and their surface morphology and average grain size were studied by FESEM. Average grain diameter were determined by intercept method described in the ASTM standard E 112-96, standard for determining grain size. Actual grain size determination as the above procedure was done with the help of image analysis software.

3. Results and discussion

3.1. Glycothermal synthesis and characteristics of $Ba(Mg_{1/3}Ta_{2/3})O_3$ nanopowders

3.1.1. Effect of reaction temperature

In order to investigate effects of the reaction temperature on the phase and morphology of glycothermally derived BMT nanoparticles, precursors were treated at different temperatures with molar ratio of Ba:(Mg + Ta) to 1.5:1 for 24 h. Fig. 2 shows XRD patterns of $Ba(Mg_{l/3}Ta_{2/3})O_3$ nanopowders glycothermally synthesized in 1,4-butanediol solution at different reaction temperatures. It is relatively straightforward to produce BMT nanopowders with the desired perovskite phase. While the main peaks in the XRD patterns shown in Fig. 2 are those for the perovskite phase, small peak may be noted at $2\theta = 25.11$, corresponds to $BaCO_3$. XRD results indicate that the products were amorphous at 90 °C and BMT phase started to form at 120 °C. Thus, the transition temperature of the amorphous precursors to crystalline solid in glycothermal condition was in the vicinity of 120 °C. $BaCO_3$ content was gradually decreased with increasing the reaction temperature, which was consistent with the FTIR data. Better crystallinity and sharper intensities of the diffraction peaks were observed with increasing the reaction temperature.

Fig. 3 shows the diffraction patterns in the range of 29–32° 2θ region at room temperature glycothermally derived BMT

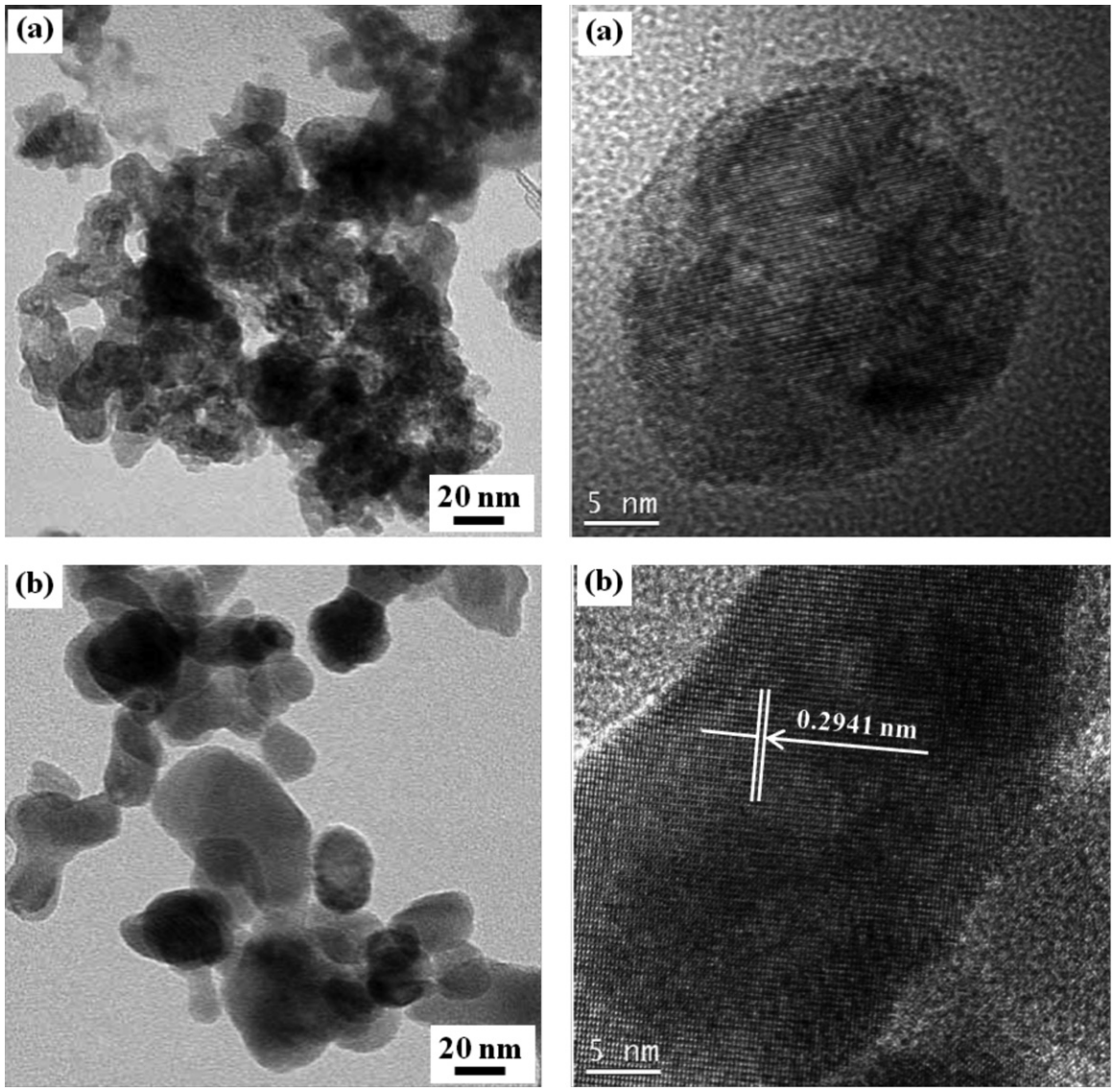

Fig. 5. TEM photomicrographs of $Ba(Mg_{1/3}Ta_{2/3})O_3$ nanopowders synthesized in glycothermal condition (24 h, Ba:Mg:Ta molar ratio of 1.5:0.33:0.67): (a) 120 °C, and (b) 220 °C.

powder. The main (1 1 0) peak is somewhat broadened. The crystallite sizes of BMT nanopowders were estimated to be changed from 10.1 to 19.7 nm with increasing the reaction temperatures from 120 to 220 °C (Table 1). These sizes agree well with the sizes determined from TEM images (from 6 ± 1 to 26 ± 5 nm).

FESEM photomicrographs of BMT nanoparticles synthesized at different temperatures are given in Fig. 4. The size and shape of BMT nanoparticles was also strongly dependent on reaction temperatures. The morphology of BMT nanoparticles gradually changed from a raspberry-like shape to round and approximately equiaxed shape with some irregularities when reaction temperature was changed from 120 °C to 220 °C. Thin hexagonal platelet particles were also observed in trace amounts in reactions conducted below 150 °C as shown in Fig. 4(b) and (c). EDS analysis of these platelets showed peaks for magnesium and oxygen but no trace of tantalum. Magnesium hydroxide has hexagonal crystal structure (JCPDS 44-1482) and is often found as hexagonal platelets.[29] Therefore, it seems likely that at least some of the magnesium not incorporated within the perovskite nanoparticles was left over and was precipitated out as the magnesium-rich phase. From these results, higher synthesis temperatures above 180 °C with coprecipitated $Mg_{1/3}Ta_{2/3}O_2 \cdot xH_2O$ improve the incorporation of magnesium into BMT to produce a homogeneous, stoichiometric powder.[30]

TEM images, shown in Fig. 5, show the raspberry-like morphology for BMT nanoparticle synthesized at 120 °C, which consist of cluster of irregularly shaped crystallites with a size of around 10 nm whereas the mono crystalline equiaxed morphology for BMT nanoparticles synthesized at 220 °C with a size of 26 ± 5 nm. BMT crystallites increase from ~10 nm to 25 nm when the reaction temperature was changed from 120 °C to 220 °C. In the glycothermal condition, the highly alkaline con-

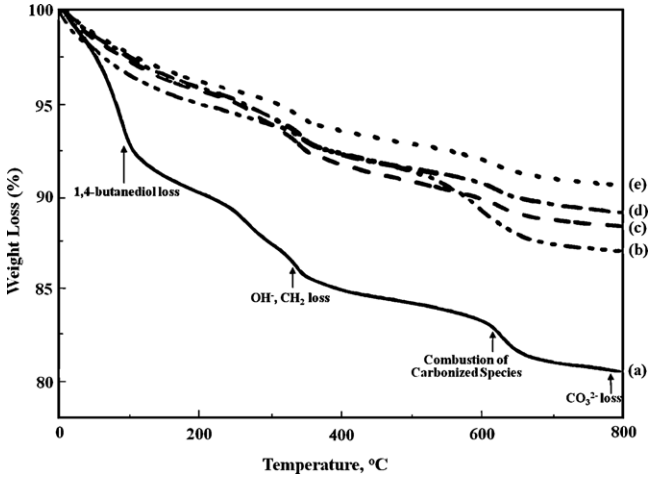

Fig. 6. Thermogravimetric analysis of $Ba(Mg_{1/3}Ta_{2/3})O_3$ nanopowders synthesized in glycothermal condition at 220 °C (24 h, Ba:Mg:Ta molar ratio of 1.5:0.33:0.67).

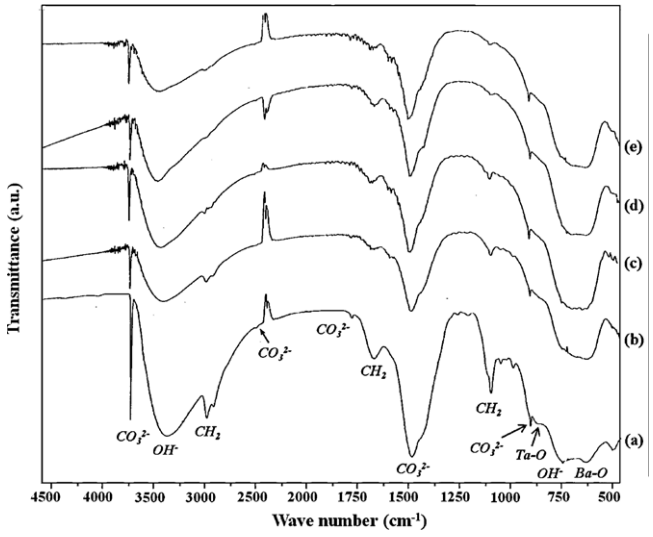

Fig. 7. FTIR spectra of $Ba(Mg_{1/3}Ta_{2/3})O_3$ nanopowders synthesized in glycothermal condition at various reaction temperatures (24 h, Ba:Mg:Ta molar ratio of 1.5:0.33:0.67): (a) 90 °C, (b) 120 °C, (c) 150 °C, (d) 180 °C, and (e) 220 °C.

ditions as in aqueous solution are not necessary for the formation of BMT nanoparticles in glycothermal reaction. Therefore, this process eliminate the need for the alkaline mineralizer from the final products.[31]

The as-prepared BMT powder was investigated by TGA and FTIR measurements to look for impurities such as water or organic species. Fig. 6 shows TGA analysis of BMT nanoparticles synthesized at different reaction temperatures. The total weight losses synthesized at 90, 120, 150, 180, and 220 °C for 24 h were, respectively, 19.2, 12.8, 11.5, 10.7, and 9.3 wt%. The total weight loss between 100 and 800 °C is <12.8 wt% for the powder synthesized at 120 °C and decreases significantly with increasing synthesis temperatures, becoming <9.3 wt% at 220 °C. The total weight loss consists of four contributions. The first region (<200 °C) corresponds to the loss of physically adsorbed water and 1,4-butanediol. The second region between 200 and 350 °C corresponds to the loss of chemically bound hydroxyl groups. The weight loss of the third regions between 350 and 700 °C is attributed to the combustion of carbonized species by 1,4-butanediol chemically bounded inside BMT nanoparticles and on the surface. Finally, the weight loss above 700 °C is due to CO_2 release from decomposition of carbonate species.[32] From the TGA analysis, it is found that the hydroxyl, chemically bound l,4-butanediol, and carbonate content decreased with increasing synthesis temperature.

The TGA results were consistent with the FTIR analysis. FTIR spectra of BMT nanopowder synthesized at different reaction temperatures are given in Fig. 7. The absorption peak between 1582 and 1432 cm^{-1} is due to the asymmetric stretching of the carbonates ion impurities ($BaCO_3$), its maximum is observed at 1496 cm^{-1}.[33] Also, the sharp peaks at 910, 1791, 2497 and 3741 cm^{-1} are also characteristic of the CO_3^{2-} group.[33] The strong band at 743 cm^{-1} is characteristic of librational mode of OH^- groups and is more distinct than the OH^- stretching which is masked by the corresponding H_2O bands around 3375 cm^{-1}.[33] Bound hydroxyls are invariably found on a surface of solvothermally derived powder due to surface hydration by residual H_2O of precipitated hydrous oxide and are most commonly removed by heating.[33] The data does reveal weak shoulders near 2968, 2906, 1682, and 1109 cm^{-1}, which are characterized by the adsorption of CH_2 groups. Chemical adsorption and entrapment with the particles of 1,4-butanediol is believed to be involved in the formation of these peaks through substitution on a surface hydroxyl group.[34,35] The weak shoulder at around 875 cm^{-1} may have arisen from Ta–O vibrations since there are a number of vibrations recorded for Ta–O in the region 880–940 cm^{-1}. The low intensity of the vibration could have been reduced by the effect of the crystalline lattice.[36,37] The broad band peak at 625 cm^{-1} with a shoulder at around 650–680 cm^{-1} may be substantially the result of Ba–O vibrations because the Ba–O bond vibrates at about 635 cm^{-1}.[38] FTIR analysis suggest that several defects are present in the surface of BMT crystallites. Intensities of all absorption bands for these surface defects decreased with increasing the reaction temperature and have minimum at 220 °C.

3.1.2. *Effect of reaction time*

The reaction time plays an important role in the phase transformations from amorphous MTO hydrous gel to BMT phase. The effect of reaction time (1–24 h) was studied under the synthesis condition of 220 °C, Ba:(Mg + Ta) = 1.5. The XRD patterns and SEM of the powders synthesized at different glycothermal reaction times are given in Figs. 8 and 9, respectively. Fig. 9(a) shows the characteristics of MTO hydrous gel. The amorphous MTO hydrous gel exhibits a fine, porous network structure, which is believed to be infiltrated by 1,4-butanediol as shown in Fig. 9(a). The interconnected network structure was experimentally observed by both the large surface area obtained via nitrogen adsorption technique (≈300 m^2/g). EDS analysis of MTO hydrous gel showed peaks for magnesium, tantalum, and oxygen with almost stoichiometric ratio. The phase transformation from MTO hydrous gel with $Ba(OH)_2 \cdot 8H_2O$ to BMT

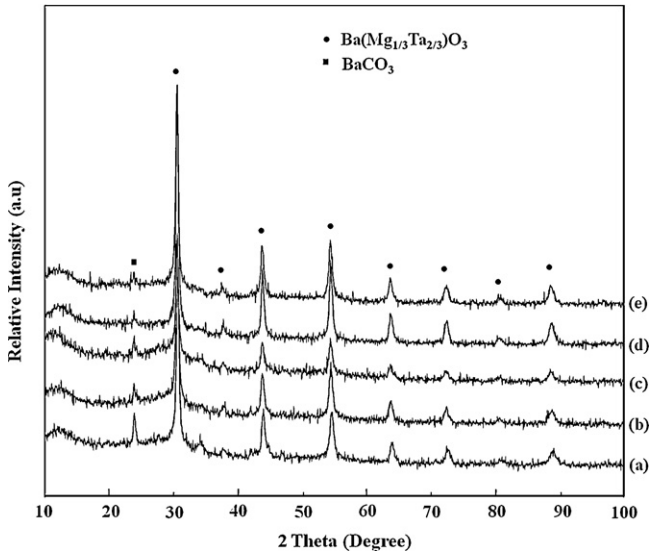

Fig. 8. XRD patterns of $Ba(Mg_{1/3}Ta_{2/3})O_3$ nanopowders synthesized in glycothermal condition at various reaction times (220 °C, Ba:Mg:Ta molar ratio of 1.5:0.33:0.67): (a) 1 h, (b) 3 h, (c) 6 h, (d) 12 h, and (e) 24 h.

phase is shown in Fig. 8(a)–(e). The phase transformation from MTO gel to BMT phase very rapidly occurs within 1 h as shown in Fig. 8(a). This conversion to BMT phase is illustrated in the SEM photomicrographs shown in Fig. 9(b)–(f). There is no distinct morphology change of BMT nanoparticles and the intensity of XRD patterns slightly increased when the reaction time increased from 1 h to 24 h. It was observed that magnesium-rich phase appears at the early stage of reaction and partial precipitation of these thin hexagonal platelet particles from NTO hydrous gel occurs with an induction period of 1 h as shown in Figs. 8(a) and 9(b). It is observed that magnesium-rich phase disappeared when the reaction time increased from 6 h to 12 h. Therefore, it also seems likely that at least some of the magnesium were precipitated out as the magnesium-rich phase from MTO gel at the early stage of reaction. Longer reaction time than 12 h facilitates the incorporation of magnesium into BMT to produce a homogeneous, stoichiometric powder.

3.2. *Heat-treatment of $Ba(Mg_{1/3}Ta_{2/3})O_3$ nanopowders prepared by glycothermal process*

To examine the effects of the reaction temperature and time on stoichiometry and homogeneity, BMT nanoparticles were heat-treated at 1100 °C for 4 h, which was generally used for synthesis of BMT powder in solid-state reaction.[13,15] The diffraction patterns of $Ba(Mg_{1/3}Ta_{2/3})O_3$ nanopowders heat-treated at 1100 °C for 4 h are given in Figs. 10 and 11. When the reaction temperature was below 220 °C, the $Ba_3Ta_5O_{15}$ phase was found as shown in Fig. 10. The intensity of the peak decreased with increasing the reaction temperature. Homogeneous and stoichiometric BMT phase without contamination of $Ba_3Ta_5O_{15}$ phase were only observed when the reaction temperature for glycothermal synthesis of BMT nanoparticles was 220 °C. When the reaction time was less than 12 h, the $Ba_3Ta_5O_{15}$ phase was also found even if reaction temperature was 220 °C as shown in Fig. 11. The intensity of the peak decreased with increasing the reaction time. Homogeneous and stoichiometric BMT phase without contamination of $Ba_3Ta_5O_{15}$ phase were observed when the reaction time for glycothermal synthesis of BMT nanoparticles was longer than 12 h at 220 °C. It had been suggested from

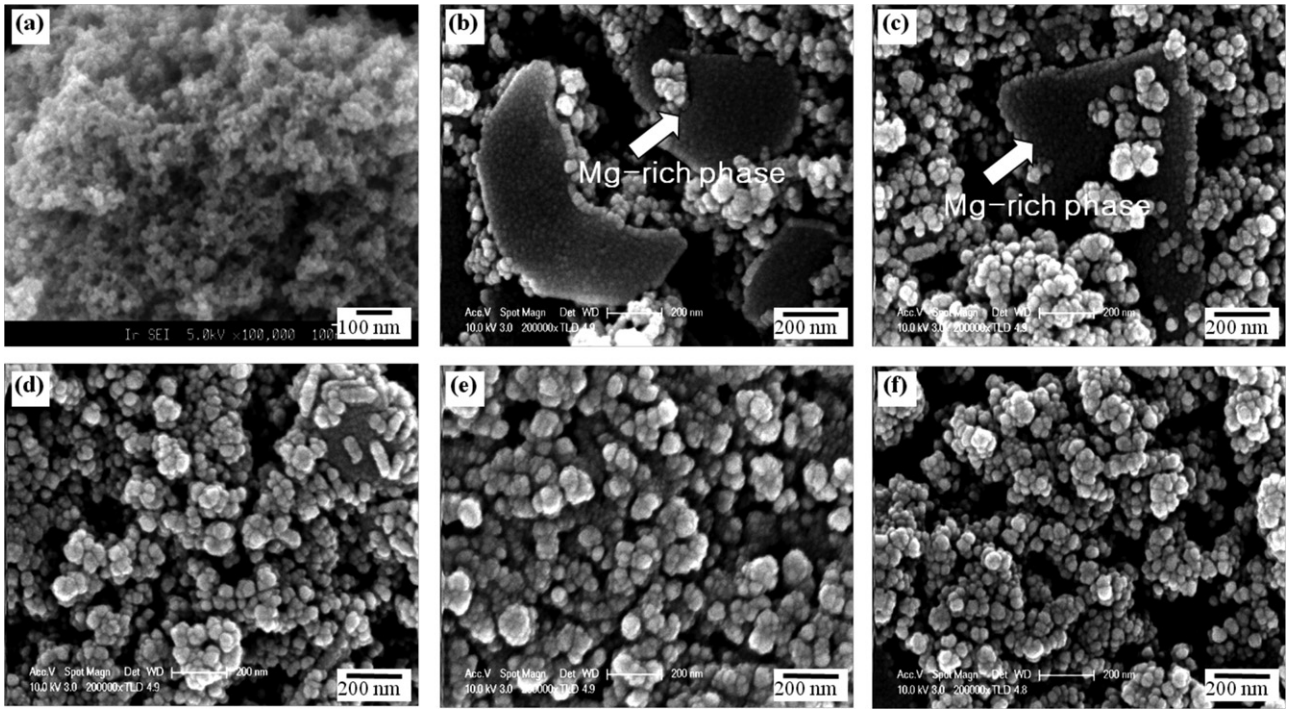

Fig. 9. SEM photomicrographs of $Ba(Mg_{1/3}Ta_{2/3})O_3$ nanopowders synthesized in glycothermal condition at various reaction times (220 °C, Ba:Mg:Ta molar ratio of 1.5:0.33:0.67): (a) MTO gel, (b) 1 h, (c) 3 h, (d) 6 h, (e) 12 h, and (f) 24 h.

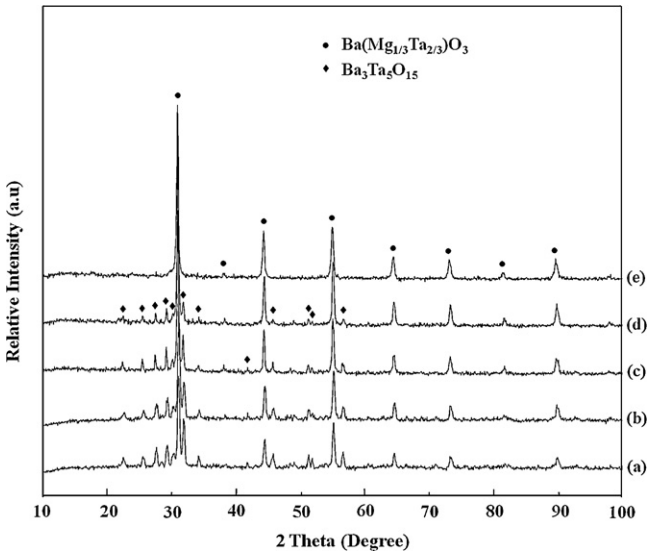

Fig. 10. XRD patterns of $Ba(Mg_{1/3}Ta_{2/3})O_3$ nanopowders calcined at 1100 °C for 4 h: (a) 90 °C, (b) 120 °C, (c) 150 °C, (d) 180 °C, and (e) 220 °C.

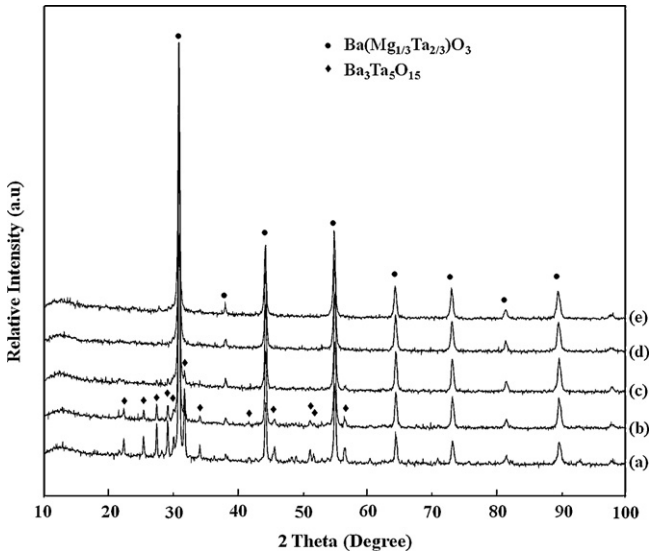

Fig. 11. XRD patterns of $Ba(Mg_{1/3}Ta_{2/3})O_3$ nanopowders calcined at 1100 °C for 4 h: (a) 1 h, (b) 3 h, (c) 6 h, (d) 12 h, and (e) 24 h.

these XRD data that the preparation of BMT nanopowder with desired stoichiometry and homogeneity is more difficult while perovskite BMT phase may be produced readily by glycothermal synthesis without alkaline mineralizer. It seems likely that when the reaction temperature was below 180 °C and the reaction time was less than 12 h, the magnesium does not fully react with the other ions for the formation of stoichiometric BMT phase by leaving some magnesium in solution as magnesium-rich phase. Some unreacted magnesium-rich phase is probably precipitated out as the hexagonal platelets on cooling after glycothermal reactions, which can be observed in samples with the reaction temperature below 220 °C and the reaction time less than 12 h. This magnesium-rich phase roughly explained the formation of $Ba_3Ta_5O_{15}$ phase[30] when the magnesium-deficient BMT nanoparticles were heat-treated at 1100 °C.

SEM photomicrographs of BMT nanopowders obtained after heat-treatment of 1100 °C for 4 h are given in Fig. 12. It reveals that the heat-treated BMT powders are agglomerated by the primary particle of 60–100 nm and the diameter of agglomerates is 100–200 nm. Therefore, it is demonstrated that the key to the synthesis of a stoichiometric BMT powder is the optimum synthesis temperature that the magnesium reacts fully with the barium and tantalum ions in glycothermal reaction. However, more work such as Ba:Mg:Ta molar ratio and the reaction media is required in order to achieve the desired goal of producing a homogeneous BMT nanopowder in a reproducible manner.

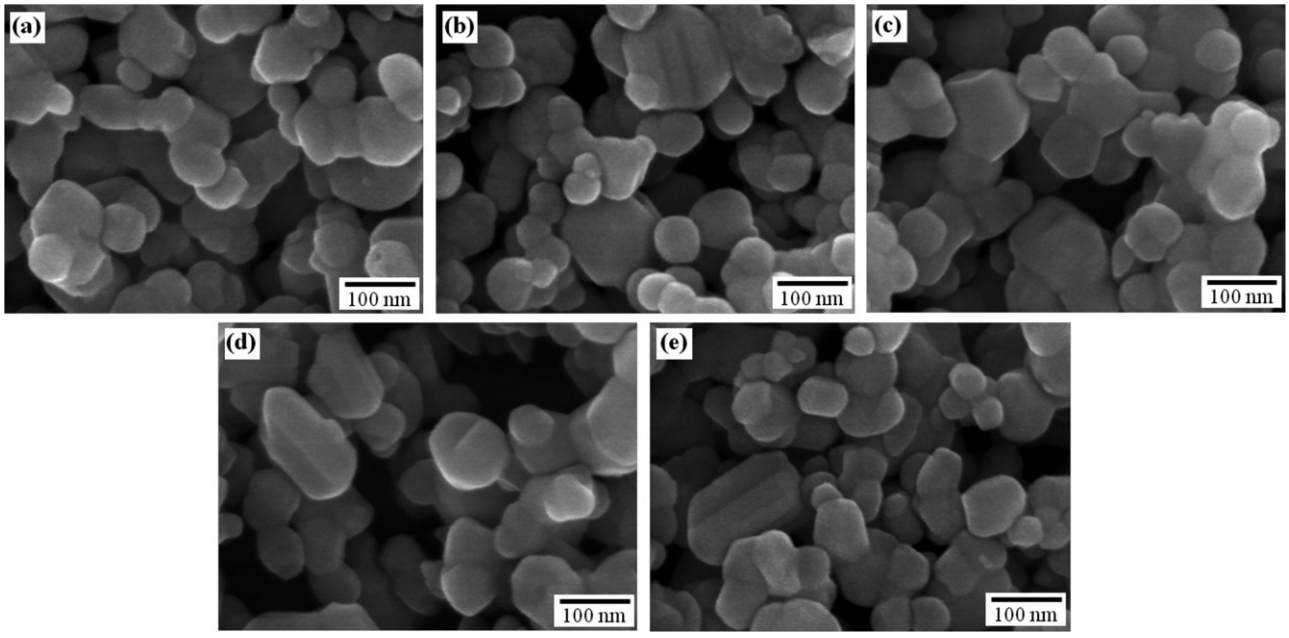

Fig. 12. SEM photomicrographs of $Ba(Mg_{1/3}Ta_{2/3})O_3$ nanopowders calcined at 1100 °C for 4 h: (a) 90 °C, (b) 120 °C, (c) 150 °C, (d) 180 °C, and (e) 220 °C.

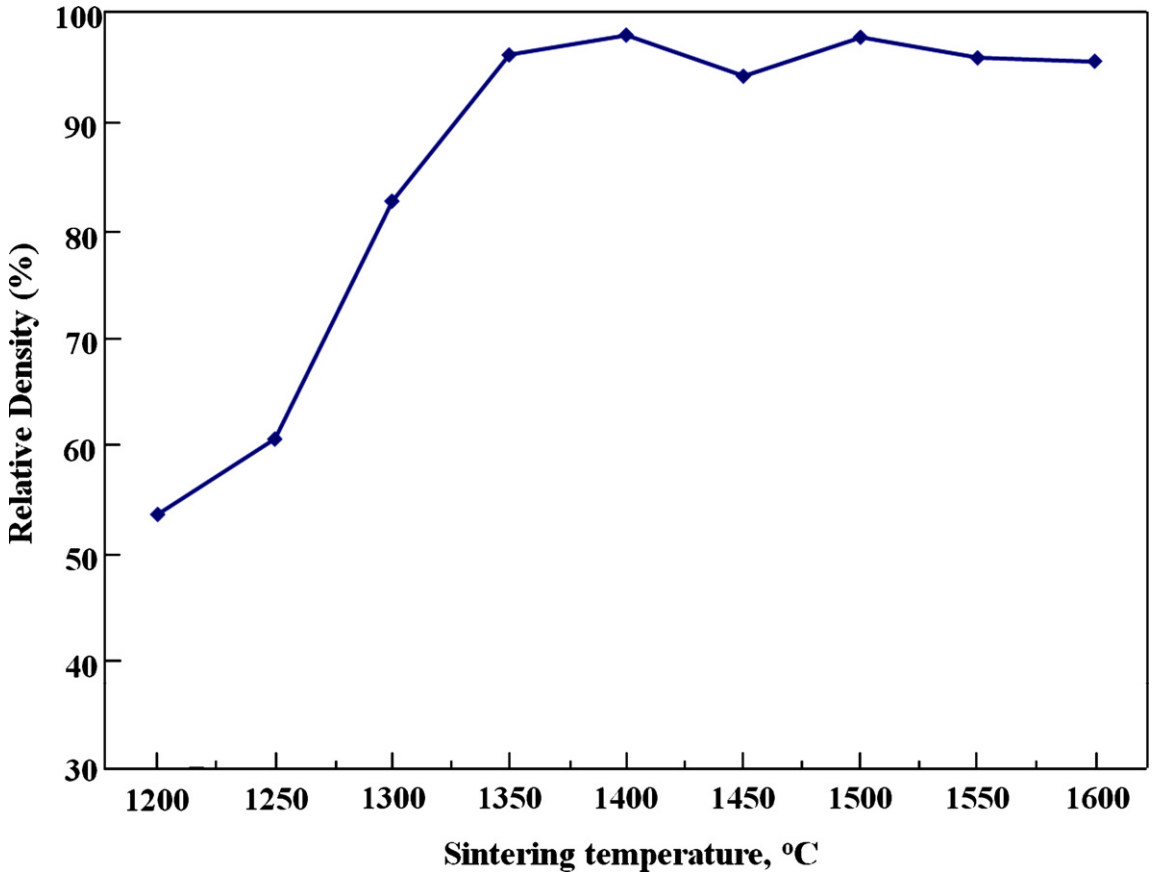

Fig. 13. Variation of sintered density for the $Ba(Mg_{1/3}Ta_{2/3})O_3$ ceramics derived from glycothermal $Ba(Mg_{1/3}Ta_{2/3})O_3$ nanopowders as a function of sintering temperature (10 h).

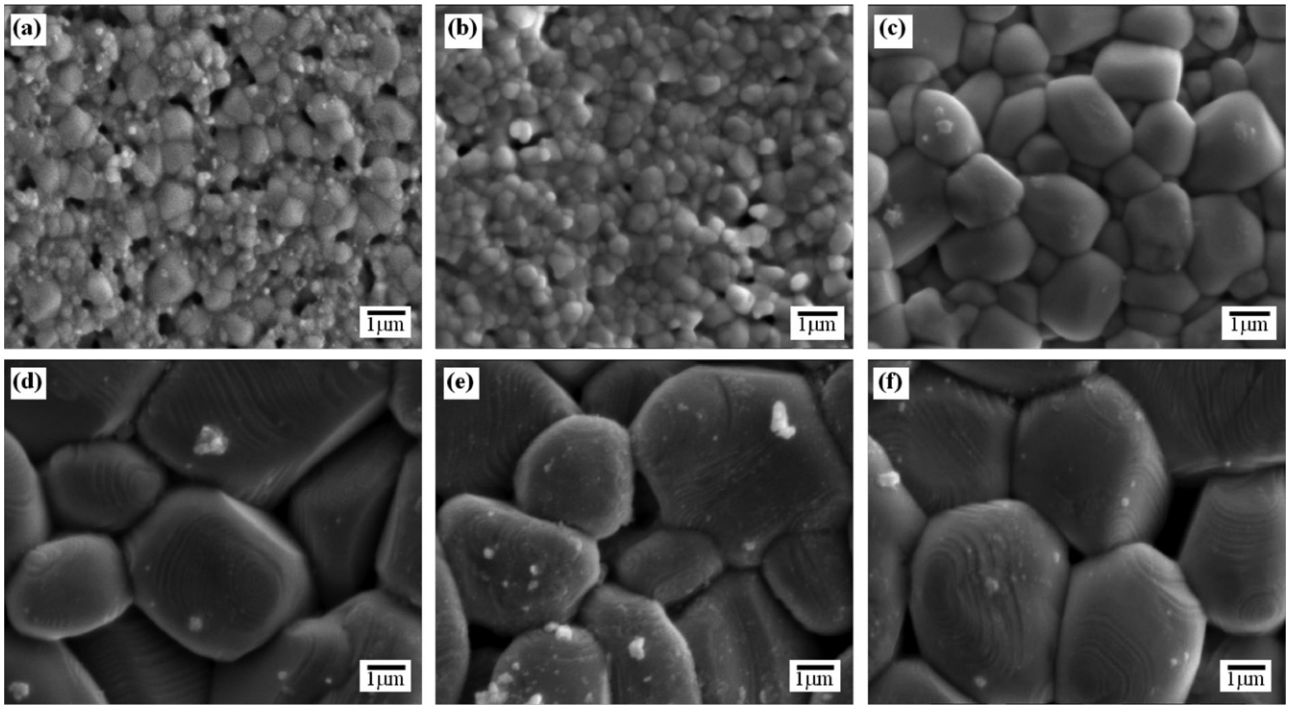

Fig. 14. SEM photomicrographs of $Ba(Mg_{1/3}Ta_{2/3})O_3$ ceramics sintered at (a) 1250 °C, (b) 1300 °C, (c) 1350 °C, (d) 1400 °C, (e) 1450 °C, and (f) 1600 °C.

3.3. Densification of $Ba(Mg_{1/3}Ta_{2/3})O_3$ ceramics

The powders obtained at 220 °C contain some portion of agglomerate with small particles. Since the agglomeration was sufficiently small and soft, there was no need for a milling process with dispersant. During compaction, the powders are easily formed into homogeneous green compacts. The as-received BMT nanopowder was uniaxially pressed 150 MPa to make green bodies, followed by sintering at temperatures from 1200 to 1600 °C in air for 10 h. Fig. 13 shows the effects of sintering temperature on the bulk density of the sintered bodies. The bulk density increases from 53.4% at 1200 °C to 98.5% at 1400 °C. Sintering below 1250 °C showed little densification for glycothermally derived BMT nanopowder. Increasing the sintering temperature to above 1450 °C does not result in more highly densified BMT ceramics (96.4% of the theoretical density at 1600 °C). A very high density of 97.67% can be achieved at sintering temperature as low as 1350 °C for 10 h. BMT ceramics with similar high density has been attained by Kolodyazhnyi et al.[30] using a solid-state method, but sintering at 1600 °C for duration of 20 h was needed. Based on these results, it is demonstrated that glycothermally derived BMT nanopowder is very reactive and can significantly reduced sintering temperature from 1600 to 1350 °C.

The microstructural evolutions of BMT ceramics sintered at different temperatures are shown in Fig. 14. The microstructure of BMT ceramics sintered between 1250 and 1600 °C are essentially composed by polyhedral grains. Significant densification and grain growth progressed as the sintering temperature increased from 1250 to 1300 °C as shown in Fig. 14(a) and (b). As it can be observed, uniform microstructure was developed with a relatively slow grain growth up to 83.77% of the theoretical density. In this stage sintering, pores between grains are almost closed and a quite fine-grained matrix developed with an uniform distribution of grain size (0.4 ± 0.2 μm). After heat treatment at 1350 °C, the microstructure starts to be bimodal with some relatively large grains (>1.5 ± 0.2 μm) growing in a fine-grained matrix (<0.7 ± 0.2 μm) although the samples are near fully dense as shown in Fig. 14(c). When the sintering temperature increased from l350 to 1400 °C, the grain size of the BMT ceramics increased from 1.2 ± 0.2 μm to 3.5 ± 1 μm and the BMT sintered body has maximum density of 98.46% as shown in Fig. 14(d). Some large open pores started to be developed within the large grains above 1450 °C, which reduced the density of the BMT sintered bodies as shown in Fig. 14(e) and (f).

4. Conclusion

A new glycothermal process has been developed for synthesizing phase-pure $Ba(Mg_{l/3}Ta_{2/3})O_3$ nanopowders using l,4-butanediol as the reaction medium in glycothermal environment. The phase purity of $Ba(Mg_{1/3}Ta_{2/3})O_3$ significantly depends on the reaction temperature. Well crystallized phase-pure perovskite $Ba(Mg_{1/3}Ta_{2/3})O_3$ was successfully produced at as low as 220 °C. The average particle size of the as-prepared powder was 26 ± 5 nm. It is also demonstrated that glycothermally derived BMT nanopowder is very reactive and can significantly reduced sintering temperature from 1600 to 1350 °C. BMT ceramics with high density of 97.67% can be obtained at sintering temperature as low as 1350 °C for 10 h. The developed glycothermal process is considered to be a highly potential method for synthesizing complex ceramic powders such as $Ba(Mg_{l/3}Ta_{2/3})O_3$ and $Ba(Zn_{1/3}Ta_{2/3})O_3$ at relatively low temperature.

References

1. Yoon KH, Kim DP, Kim ES. Effect of $BaWO_4$ on the microwave dielectric properties of $Ba(Mg_{1/3}Ta_{2/3})O_3$ ceramics. *J Am Ceram Soc* 1994;**77**(4):1062–6.
2. Nomura S, Toyama K, Kaneta K. $Ba(Mg_{1/3}\ Ta_{2/3})O_3$ ceramics with temperature-stable high dielectric constant and low microwave loss. *Jpn J Appl Phys* 1982;**21**:L624–6.
3. Kawashima S, Nishida M, Ueda I, Ouchi H, Hayakawa S. Dielectric properties of $Ba(Zn_{1/3}Nb_{2/3})O_3$–$Ba(Zn_{1/3}Ta_{2/3})O_3$ ceramics. *Proc Ferroelectr Mater Appl* 1977;**1**:293.
4. Kawashima S, Nishida M, Ueda I, Ouchi H. $Ba(Zn_{1/3}Ta_{2/3})O_3$ ceramics with low dielectric loss at microwave frequencies. *J Am Ceram Soc* 1983;**66**(6):421–3.
5. Sagala DA, Koyasu S. Infrared reflection of $Ba(Mg_{1/3}Ta_{2/3})O_3$ ceramics. *J Am Ceram Soc* 1993;**76**(10):2433–6.
6. Siny IG, Tao R, Katiyar RS, Guo R, Bhalla AM. Raman spectroscopy of Mg–Ta order–disorder in $Ba(Mg_{1/3}Ta_{2/3})O_3$. *J Phys Chem Solids* 1998;**59**:181–95.
7. Wakino K, Murata M, Tamura H. Far infrared reflection spectra of $Ba(Zn,Ta)O_3$–$BaZrO_3$ dielectric resonator material. *J Am Ceram Soc* 1986;**69**(1):34–7.
8. Matsumoto H, Tamura H, Wakino K. $Ba(Mg_{1/3}Ta_{2/3})O_3$–$BaSnO_3$ high-Q dielectric resonator. *Jpn J Appl Phys* 1991;**30**:2347–9.
9. Matsumoto K, Hiuga T, Takada K, Ichimura H. $Ba(Mg_{l/3}Ta_{2/3})O_3$ ceramics with ultra-low loss at microwave frequencies. In: *Proceedings of the sixth international symposium on applications of ferroelectrics (June, 1986)*. New York: IEEE; 1986. p. 118–21.
10. Kwon KH, Han SM, Nahm S, Kim MH, Kim YS. Compact hairpin-shaped duplexer using a BMT substrate with high dielectric constant. *Microw Opt Technol Lett* 2004;**41**(4):251–3.
11. Cheng CM, Hsieh YT, Yang CF. The sintering and microwave dielectric characteristics of MgO–CaO–Al_2O_3–SiO_2 glass-fluxed $Ba(Mg_{1/3}Ta_{2/3})O_3$ ceramics. *Mater Lett* 2003;**57**:1471–6.
12. Davies PK. Influence of structural defects on the dielectric properties of ceramic microwave resonators. In: Negas T, Ling H, editors. *Ceramic transactions, vol. 53, materials and processes for wireless communications.*. Westerville, OH: American Ceramic Society; 1995. p. 137–52.
13. Huang CL, Chiang KH, Chuang SC. Influence of V_2O_5 additions to $Ba(Mg_{1/3}Ta_{2/3})O_3$ ceramics on sintering behavior and microwave dielectric properties. *Mater Res Bull* 2004;**39**:629–36.
14. Tien LC, Chou CC, Tsai DS. Ordered structure and dielectric properties of lanthanum-substituted $Ba(Mg_{1/3}\ Ta_{2/3})O_3$. *J Am Ceram Soc* 2000;**83**(8):2074–8.
15. Tien LC, Chou CC, Tsai DS. Microstructure of $Ba(Mg_{1/3}Ta_{2/3})O_3$–$BaSnO_3$ microwave dielectrics. *Ceram Int* 2000;**26**:57–62.
16. Lu CH, Tsai CC. Homogeneous precipitation synthesis and sintering behavior of microwave dielectrics: $Ba(Mg_{/3}Ta_{2/3})O_3$. *Mater Sci Eng B* 1998;**55**:95–101.
17. Chen XM, Wu Y1. Dielectric characteristics of $Ba(Mg_{1/3}Ta_{2/3})O_3$ ceramics sintered at low temperatures. *J Mater Sci Mater Electron* 1996;**7**:369–71.
18. Renoult O, Boilot JP, Chaput F, Papiernik R, Hubert-Pfalzgraf LG, Lejeune M. Sol–gel processing and microwave characteristics of $Ba(Mg_{1/3}Ta_{2/3})O_3$ dielectrics. *J Am Ceram Soc* 1992;**75**(12):3337–40.
19. Kell RC, Greenham AC, Olds GCE. High-permittivity temperature-stable ceramic dielectrics with low microwave loss. *J Am Ceram Soc* 1973;**56**(7):352–4.

20. Kakegawa K, Wakabayashi T, Sasaki Y. Preparation of $Ba(Mg_{1/3}Ta_{2/3})O_3$ by using oxine. *J Am Ceram Soc* 1986;**69**(4):C82–3.
21. Maclaren I, Ponton CB. Low temperature hydrothermal synthesis of $Ba(Mg_{1/3}Ta_{2/3})O_3$ sol-derived powders. *J Mater Sci* 1998;**33**:17–22.
22. Lencka MM, Anderko A, Riman RE. Hydrothermal precipitation of lead zirconate titanate solid solutions: thermodynamic modeling and experimental synthesis. *J Am Ceram Soc* 1995;**78**(10):2609–18.
23. Inoue M. Glycothermal synthesis of metal oxides. *J Phys Condens Matter* 2004;**16**:S1291–303.
24. Cho SB, Venigalla S, Adair JH. Morphological forms of a-alumina particles synthesized in 1,4-butanediol solution. *J Am Ceram Soc* 1996;**79**(1):88–96.
25. Bell NS, Adair JH. Adsorbate effects on glycothermally produced a-alumina particle morphology. *J Cryst Growth* 1999;**203**:213–26.
26. Inoue M, Nishikawa T, Otsu H, Kominami H, Inui T. Synthesis of rare-earth gallium garnets by the glycothermal method. *J Am Ceram Soc* 1998;**81**(5):1173–83.
27. Dey SK, Lee JJ. Cubic paraelectric (nonferroelectric) perovskite PLT thin films with high permittivity for ULSI DRAM's and decoupling capacitors. *IEEE Trans Electron Devices* 1992;**39**(7):1607–13.
28. Cullity BD, Stock SR. *Elements of X-ray diffraction*. 3rd ed. Englewood Cliffs, NJ: Prentice-Hall; 2001, 622 pp.
29. Itatani K, Koizumi K, Howell FS, Kishioka A, Kinoshita M. Agglomeration of magnesium oxide particles formed by the decomposition of magnesium hydroxide. *J Mater Sci* 1989;**24**(7):2603–9.
30. Kolodyazhnyi TV, Petric A, Johari GP, Belous AG. Effect of preparation conditions on cation ordering and dielectric properties of $Ba(Mg_{1/3}Ta_{2/3})O_3$ ceramics. *J Eur Ceram Soc* 2002;**22**:2013–21.
31. Kim BK, Lim DY, Riman RE, Nho JS, Cho SB. A new glycothermal process for barium titanate nanoparticle synthesis. *J Am Ceram Soc* 2003;**86**(10):179396.
32. Newalkar BL, Komarneni S, Katsuki H. Microwave-hydrothermal synthesis and characterization of barium titanate powders. *Mater Res Bull* 2001;**36**:2347–55.
33. Duraán P, Gutierrez D, Tartaj J, Banares MA, Moure C. On the formation of an oxycarbonate intermediate phase in the synthesis of $BaTiO_3$ from (Ba,Ti)-polymeric organic precursors. *J Eur Ceram Soc* 2002;**22**: 797–807.
34. Morrow BA. Vibrational spectroscopies for adsorbed species. *ACS symposium series*, vol. 137. Washington, DC: American Chemical Society; 1980. p. 119.
35. Jung YJ, Lim DY, Nho JS, Cho SB, Riman RE, Lee BW. Glycothermal synthesis and characterization of tetragonal barium titanate. *J Cryst Growth* 2005;**274**:638–52.
36. Nakamoto K. Part II. Inorganic compounds. In: *Infrared and Raman spectra of inorganic and coordination compounds*. 4th ed. New York: Wiley-Interscience; 1986. p. l06.
37. Weltner Jr W, McLeod Jr D. Spectroscopy of TaO and TaO_2 in neon and argon matrices at 4° and 20 °K. *Chem Phys* 1965;**42**(3): 882–91.
38. Mishra D, Anand S, Panda RK, Das RP. Characterization of products obtained during formation of barium monoaluminate through hydrothermal precipitation-calcination route. *J Am Ceram Soc* 2002;**85**(2): 437–43.